ELSEVIER

Journal of Alloys and Compounds 253–254 (1997) 62–65

Journal of ALLOYS AND COMPOUNDS

Electron emission at the surface of metal tritide films

N.P. Kherani[a,*], W.T. Shmayda[a], J.M. Perz[b], K.G. McNeill[b], S. Zukotynski[c]

[a]*Ontario Hydro Technologies, 800 Kipling Avenue, Toronto, Canada M8Z 5S4*
[b]*University of Toronto, Department of Physics, Toronto, Canada M5S 1A7*
[c]*University of Toronto, Department of Electrical and Computer Engineering, Toronto, Canada M5S 3G4*

Abstract

Monte Carlo simulations of tritium decay electrons in three metal tritide films, LiT, MgT_2 and TiT_2, of effectively infinite thickness have been performed to determine distributions of the total electron energy and the normal energy E_n at the surface of these materials. Monte Carlo calculations of electron emission at the surface of an effectively infinite 'slab' of tritium gas (STP) have also been carried out. Using a planar retarding potential analyzer, measurement of the integrated electron flux and the distribution of normal energies E_n from 50 eV to 7.4 keV have been carried out for lithium tritide films of effectively infinite thickness prepared with various tritium to lithium atomic ratios. A comparison of the measured and computed distributions shows that the measured flux is greater than the computed result for E_n below approximately 1.5 keV, while for E_n above 1.5 keV the two distributions are in good agreement. Calculations of high energy secondary and Auger electron contributions suggest that the observed discrepancy at lower energies can be largely accounted for by Auger electrons associated with impurities in the near-surface region of the lithium tritide films.

Keywords: Tritium; Metal tritide; Monte Carlo; Electron emission; Electron propagation

1. Introduction

In the last several years there has been a growing interest in exploring the potential for using metal tritides for the purpose of radioluminescent lighting. This interest is motivated largely by the need for radioluminescent light structures that can hold tritium in a solid matrix as opposed to the traditional and more potentially hazardous tritium gas in a phosphor-coated glass tube, and the need for light structures that are brighter than the common tritium gas-filled glass tubes. In an attempt to address these concerns, a program at the research laboratories of Ontario Hydro was initiated with the objective of examining advanced tritium-based radioluminescent light structures. During the early stages of this program it was recognized that there were several solid media in which tritium could be occluded. It was also recognized that an understanding of the propagation of tritium decay electrons through condensed media and the emission of electrons at the surface of tritiated solids was essential to a proper investigation of tritium occluders and thus would play a significant role in the development of any such radioluminescent light structure. Furthermore, this understanding would also be useful in the areas of tritium imaging studies of first-wall fusion reactor materials and dosimetric studies dealing with the hazard of inhalation of metal tritide particulates.

With the foregoing motivating factors at heart, and noting that while the physics of electron-matter interaction has been studied both theoretically and experimentally [1–8] reported investigations of tritium decay betas traversing metal tritide films are quite scarce and undetailed [9], the objective of this study is to examine the propagation of tritium decay betas and subsequent emission from metal tritide films.

This paper presents the results of Monte Carlo calculations of the electron energy distribution at the surface of effectively infinitely thick metal tritide films, describes experimental measurements of the electron flux and energy distribution at the surface of lithium tritide, and compares the experimental data with the Monte Carlo results for LiT. The Monte Carlo results for electron emission at the surface of an effectively infinitely thick 'slab' of tritium gas (STP) are also given.

2. Monte carlo calculations

The fundamental principle of a Monte Carlo electron trajectory simulation is a stepwise representation of the path of an electron, taking into account both elastic and

*Corresponding author

0925-8388/97/$17.00
PII S0925-8388(96)03086-1

inelastic scattering events [6]. The objective of the present simulation was to attempt to describe the path of an electron, which had its origin in the decay of a tritium atom, through a thin metal tritide film until it either was absorbed or crossed one of the film surfaces. Physical models were developed and suitably cast into probabilistic terms to determine the distance between scattering events, the scattering angles, and the rate of energy loss. Then random number generators were used to sample from representative probability distributions and thus the trajectory of an electron through the solid was determined. This calculation procedure was repeated between 10^5 and 10^6 times to obtain a solution that was expected to approximate closely the actual steady state situation.

Because elastic scattering events, as opposed to inelastic ones, are primarily responsible for changing the direction of flight in electron–solid interactions, the Monte Carlo simulation took account of each elastic scattering event, and applied a modification of Bethe's continuous slowing down relation to determine the loss in energy between elastic scattering events, while ignoring the minor deviations in the trajectory due to inelastic scattering events [12]. This stepwise approach, referred to as the single scattering model [13], was deemed reasonable considering that the majority of inelastic scattering events result in angular deflections of the order of 0.1° [14] while elastic scattering angles range from a few degrees to 180°. With respect to energy, the Bethe relation [4], as modified by Joy and Luo [15] to include core ionization, plasmons, and conduction electron excitations, is valid for energies as low as 50 eV; electrons degrading to energies lower than this are considered to be absorbed in the solid. This relation accounts for collisional losses; bremsstrahlung radiation losses have been shown to be four orders of magnitude smaller for the electron energies considered [8]. The generation of secondary electrons due to energy transfer from the primary electrons (tritium betas), and their trajectories through the solid and consequent contribution to the electron emission, were not included in this model. It is noted that the emission of low energy secondary electrons, typically of energies less than 50 eV, was not directly considered. We note that the Monte Carlo calculations do not involve adjustable parameters or scaling factors. A detailed discussion of the application of the Monte Carlo calculations to the analysis of electron emission from the surface of a metal tritide is provided in [11].

The calculated energy distributions of the electron flux at the surface of effectively infinitely thick[1] LiT, MgT_2, and TiT_2 films are shown in Fig. 1. Fig. 1 also includes the electron energy distribution at the surface of an effectively infinitely thick 'slab' of tritium gas (STP). The data shown in Fig. 1 represent a fit of the actual Monte Carlo data. The differential electron flux distributions as a function of energy are observed to peak around 4 keV and drop to zero with decreasing energy. The flux going to zero at very low energies is consistent with our Monte Carlo model which does not account for any secondary electron contribution. The electron flux distributions clearly show the scaling of electron emission for the various tritides and tritium gas. The maximum electron emission for the tritides is at the surface of LiT, yet this flux is about 4 times smaller than that at the surface of a 'slab' of tritium gas. The latter result is due to the greater stopping power of lithium tritide than that of tritium gas.

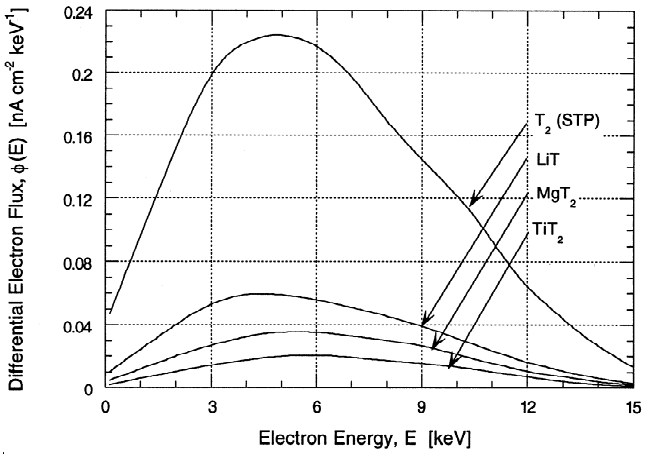

Fig. 1. Monte Carlo calculation of the energy distribution of the electron flux at the surface of the LiT, MgT_2, TiT_2 and T_2 (STP) each of effectively infinite thickness; the above curves are a smooth representation of the Monte Carlo data sets.

The integrated electron flux and the energy weighted integral of the above distributions are summarized in Table 1.

3. Experimental apparatus and procedures

The experimental system consisted of a high vacuum metal tritide film deposition chamber (base pressure at bakeout ~10^{-10} Bar) equipped with a retractable electron energy analyser and a 5-g depleted uranium bed used to store tritium. The deposition chamber included a pyrolytic

Table 1
Electron number and electron energy fluxes at the surface of LiT, MgT_2, TiT_2 and T_2 (STP), each of effectively infinite thickness

Material	$\int\phi(E)\mathrm{d}E$ (nA cm^{-2})	$\int\phi(E)E\mathrm{d}E$ (μW cm^{-2})
LiT	0.55	3.2
MgT_2	0.32	2.0
TiT_2	0.19	1.2
T_2(STP)	2.0	12.0

[1]Effectively infinitely thick is defined as a film thickness exceeding the average range of the most energetic tritium decay beta. Hence, electron emission from a film of thickness greater than the average range of 18.6 keV electrons is unchanged by increasing thickness.

graphite heater, coated with pyrolytic boron nitride. Lithium tritide films were deposited onto stainless steel substrates by evaporating 99.0% pure lithium in the presence of pure tritium gas desorbed from the heated uranium bed. A thin walled, high purity, alpha-iron liner, which does not react with lithium [10], was used as a crucible. The tritium starting pressure for each deposition was approximately 0.5 atmosphere; the quantity of tritium absorbed in the reaction was determined by measuring precisely the tritium gas pressures prior to and after the deposition. The average and minimum lithium tritide film areal densities were 0.34 and 0.19 mg cm^{-2}; the minimum density yields greater than 97% of the electron flux from an infinitely thick film.

A planar retarding potential analyser was used to measure the energy of emitted electrons. In the planar geometry the electron energy distribution is determined as a function of normal energy E_n, the kinetic energy associated with the component v_n of the electron velocity normal to the plane surface, i.e.,

$$E_n = 1/2\, mv_n^2 = 1/2\, m(|v| \cos\theta)^2 = 1/2\, E \cos^2\theta \qquad (1)$$

where v is the electron velocity, θ is the angle between the substrate normal and the velocity vector, m is the electron rest mass, and E is the electron kinetic energy.

The experimental results presented in the subsequent section are background corrected. The background current of the electron collector in the planar retarding potential analyser is of the order of a fraction of a pA. This current is largely due to betas from tritium surface contamination of the chamber walls. As a result of this background current, electron emission measurements at large values of E_n (~5 keV and above) have a significantly greater proportion of noise in the total current measurement and thus the increased scatter in the data.

4. Experimental results

4.1. Comparison with Monte Carlo calculation

Fig. 2[2] illustrates the measured distribution of electrons emitted from one of the films (corrected to unit stoichiometry) along with the Monte Carlo result for a lithium tritide film having a stoichiometry of unity and an infinite thickness. The experimental measurements over much of the energy range examined are found to be in reasonably good agreement with the Monte Carlo result. However, for E_n below about 1.5 keV, the experimental measurements show a higher flux density than the Monte Carlo calculation predicts. Correspondingly, the experimentally measured emission flux is 1.1 nA cm^{-2} while the Monte Carlo result is 0.55 nA cm^{-2}.

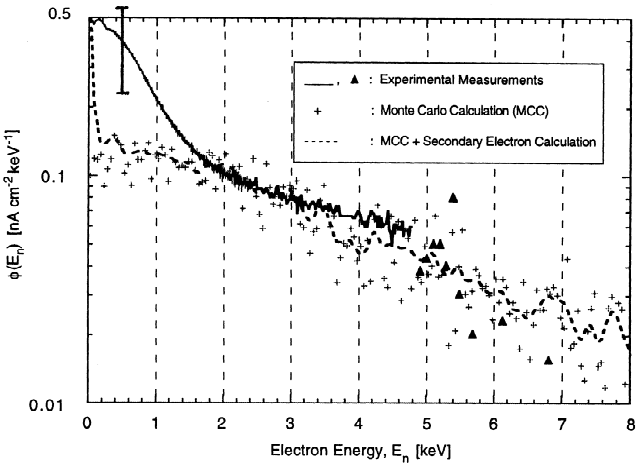

Fig. 2. Comparison of the experimentally measured distribution of electrons having energy E_n with the Monte Carlo calculation for a lithium tritide film of effectively infinite thickness; the error bar indicates the systematic uncertainty in the measurements; the contribution of high energy secondary electron calculation is also shown.

While the planar retarding potential analyser does not provide any direct measure of the angular distribution of the emission measured, one can obtain a semi-quantitative indication by measuring the electron emission as a function of the analyser to source distance. Measurements of the relative change in flux at different values of the retarding potential were carried out and found to be in reasonable agreement with the computed profile. The results suggest that the electron emission distributions, except at very low energies, $\leq$10 eV, are mainly cosine distributed, in keeping with the prediction of Monte Carlo calculations.

4.2. Contribution of high energy secondary electrons

As noted above, the Monte Carlo calculation of the electron flux at the surface of lithium tritide film was observed to be in good agreement with experimental observations for $E_n \geq 1.5$ keV, but at lower energies the calculation underestimated the flux. This discrepancy might be attributed to the fact that the calculation did not take into account secondary electron generation, but only followed the case histories of primary, tritium decay, betas. An estimate of the high energy secondary electron [16–18] contribution was computed by using the Mott–Williams quantum mechanical cross section for the interaction of slow electrons, including exchange, with atomic electrons considered as being free. The result, shown in Fig. 2, indicates that the secondary electron contribution is significant only for energies below 0.1 keV, and thus does not account for the excess electrons that appear for $0.1 < E_n < 1.5$ keV.

[2]Note that the data in this figure are presented differently from that in Fig. 1. The data in Fig. 2 are given as a function of the energy E_n, the kinetic energy associated with v_n, the component of the electron velocity normal to the plane; while the data in Fig. 1 are a function of the electron kinetic energy E.

4.3. Contribution of Auger electrons

It is known that Auger electrons are invariably produced when a sample is subjected to an external radiation source such as an electron beam. In particular, Auger electrons of characteristic energies are associated with the presence of specific elements at the surface and immediately below [19]. From a consideration of the inelastic mean free path of electrons [20], it follows that Auger electrons produced within ~30 Å of the surface are detected in Auger peaks at kinetic energies <2 keV. Auger electrons produced deeper in the sample undergo inelastic collisions and therefore can only contribute marginally to the Auger peaks; they will appear at lower kinetic energies.

In the case at hand the production of Auger electrons occurred as a result of the electron source within the lithium tritide film. The number and energy of these Auger electrons would be dictated principally by the distribution of the primary electrons, and the presence of impurity atoms in the near-surface region; the Auger energies for lithium itself are less than 50 eV. An analysis of the lithium powder used in the evaporation revealed that the dominant impurity was sodium at 0.7 atomic %. In addition the films are expected to contain some oxygen as a result of the high reactivity of lithium, and perhaps iron from the alpha-iron crucible.

The Auger current may be estimated according to the following relationship:

$$I_{\text{Auger}} = \sum I_{\text{i}} = \sum I_{\text{P}} \sigma_{\text{i}}(E_{\text{P}}) P_{\text{i}} N_{\text{i}} M_{\text{i}} \quad (2)$$

where I_{Auger} (nA cm^{-2}) is the total Auger electron current at the surface of the film, I_{i} (nA cm^{-2}) is the Auger current at the surface due to impurity i, I_{P} (nA cm^{-2}) is the primary electron current, $\sigma_{\text{i}}(E_{\text{P}})$ (cm^{2}) is the ionization cross section for a mean primary beam energy E_{P}, P_{i} is the probability of Auger emission following the ionization, N_{i} (cm^{-2}) is the areal density of a monolayer of atoms of element i, and M_{i} is the number of monolayers of element i. A calculation was carried out under the assumption that the electrons observed below 500 eV were largely due to oxygen (oxygen having an Auger peak at 503 eV). From Eq. (2) applied to oxygen [21], an estimated 3 monolayers of oxygen could generate the observed Auger current. It appears plausible that Auger electrons due to a number of impurities may be the cause of the experimental electron flux being higher than the model predictions for energies below ~1.5 keV. The plausibility of this result was confirmed experimentally [11] by systematically increasing the concentration of oxygen in the surface layers of a lithium tritide film and subsequently observing a corresponding increase in the electron flux at energies corresponding to Auger electrons due to oxygen. This is shown in Fig. 3.

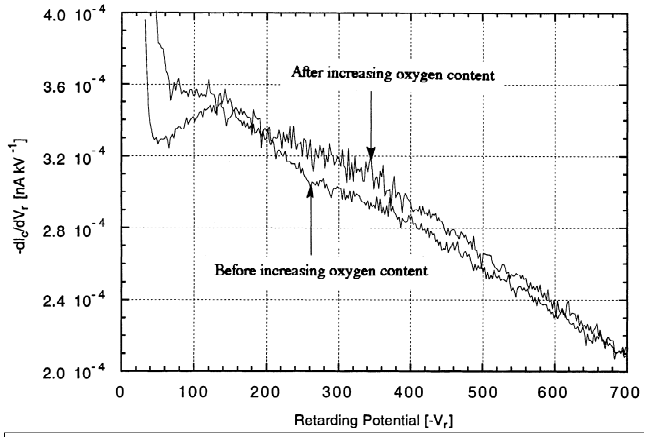

Fig. 3. Electron emission spectra showing the enhancement in the electron flux for energies less than ~500 eV due to an increase in the oxygen concentration in the surface layers of a lithium tritide film.

References

[1] N. Bohr, *Phil. Mag., (6) 25* (1913) 10.
[2] N. Bohr, *Phil. Mag., (6) 30* (1915) 581.
[3] E. Rutherford, *Phil. Mag., 21* (1911) 669.
[4] H. Bethe, *Ann. Phys., 5*, (1930) 235.
[5] H.A. Bethe and J. Ashkin, in E. Segrè (ed.), *Experimental Nuclear Physics I*, John Wiley, New York, 1953, p. 166.
[6] M.J. Berger, in B. Adle, S. Fernbach and M. Rotenberg (eds.), *Methods in Computational Physics I*, Academic, New York, 1963, p. 135.
[7] M.J. Berger and S.M. Seltzer, *Natl. Acad. Sci. Nat. Res. Council Publ., 1133* (1964) 205.
[8] R.D. Birkhoff, in S. Flugge (ed.), *Handbuch der Physik*, Vol 34, Springer, Berlin, 1955, p. 53.
[9] J.A. Tompkins, L.E. Leonard, D.B. Hawkins and R.J. Walko, in *Proceedings of Radioluminescent Lighting Technology, A Technology Transfer Conference*, Annapolis, Maryland, 1990, p. 5–1.
[10] H.C. Weed and O.H. Krikorian, *J. Nucl. Mater., 52* (1974) 142.
[11] N.P. Kherani, *Ph.D. Thesis*, University of Toronto (1994).
[12] D.E. Newbury and R.L. Myklebust, in R.H. Geiss (ed.), *Analytical Electron Microscopy*, San Francisco Press, San Francisco, 1981, p. 91.
[13] D.C. Joy, *Scanning Microscopy, 5* (1992) 329.
[14] R. Shimizu, Y. Kataoka, T. Ikuta, T. Koshikawa and H. Hashimoto, *J. Phys. D: Appl. Phys., 9* (1976) 101.
[15] D.C. Joy and S. Luo, *Scanning, 11* (1989) 176.
[16] D.C. Joy, *Microelectronic Eng., 1* (1983) 103.
[17] D.C. Joy, *J. Microscopy, 136 (2)* (1984) 241.
[18] D.C. Joy, *J. Microscopy, 147 (1)* (1987) 51.
[19] T. Sekine, Y. Nagasawa, M. Kudoh, Y. Sakai, A.S. Parkes, J.D. Geller, A. Mogami and K. Hirata, *Handbook of Auger Electron Spectroscopy*, JEOL, Tokyo, 1982.
[20] D. Briggs and M.P. Seah, *Practical Surface Analysis by Auger and X-ray Photoelectron Spectroscopy*, Wiley, New York, 1983.
[21] L.J. Kieffer and G.H. Dunn, *Rev. Mod. Phys., 38 (1)* (1966) 1.